SERI/TP-252-2337
UC Category: 62
DE84013026

Direct-Contact Condensers for Solar Pond Power Plants

Elizabeth M. Fisher
John D. Wright

July 1984

To be presented at the
ASME Winter Annual Meeting
New Orleans, Louisiana
December 1984

Prepared under Task No. 1424.10
FTP No. 153

Solar Energy Research Institute
A Division of Midwest Research Institute

1617 Cole Boulevard
Golden, Colorado 80401

Prepared for the
U.S. Department of Energy
Contract No. DE-AC02-83CH10093

Printed in the United States of America
Available from:
National Technical Information Service
U.S. Department of Commerce
5285 Port Royal Road
Springfield, VA 22161
Price:
Microfiche A01
Printed Copy A02

NOTICE

DIRECT-CONTACT CONDENSERS FOR SOLAR POND POWER PLANTS

Elizabeth M. Fisher
John D. Wright
Solar Energy Research Institute
Golden, Colorado

ABSTRACT

Direct-contact condensers for an organic Rankine cycle solar pond power plant are compared with conventional shell-and-tube condensers. Three types of direct contact systems are evaluated: drop type, bubble type, and packed columns. Methods used in the design of the direct contact systems are reviewed. Complete 5 MW_e plants, including the solar pond, are designed for each system, and their capitalized costs compared. Direct contact condensers were found to be considerably less expensive than shell-and-tube condensers. However, the auxiliary equipment needed to prevent the buildup of noncondensables and to control working fluid losses negated much of the cost savings. Also, the direct contact systems were less efficient. Thus no significant advantages were found for the direct contact condenser systems.

NOMENCLATURE

H	Henry's constant, ppm/atm
$\dot{m}$	mass flow rate, kg/s
P	pressure, Pa
V	velocity, m/s
X	concentration, ppm
Z	height, m

Subscripts

a	air
da	deaerator
eq	equilibrium
l	lateral
T	terminal

INTRODUCTION

A solar pond coupled to an organic Rankine cycle power plant converts sunlight first to heat and then to electricity. Because the temperature difference between the pond storage zone and ambient is small (<100°C) the Rankine cycle efficiency is low. Under typical operating conditions, approximately 90% of the heat removed from the solar pond must be rejected. Therefore, shell-and-tube heat exchangers account for a large fraction of the plant's capital cost. Wright (1) investigated the possibility of replacing the conventional shell-and-tube preheater/boiler with a direct-contact heat exchanger in a pentane Rankine cycle and found that it reduced the plant cost by 25%. This paper examines the feasibility of using a direct-contact condenser as well as a boiler in this application. Reference (2) contains a more detailed description of this evaluation.

SYSTEM DESCRIPTION

Three types of direct-contact condensers are sized for a 5-MW_e plant and compared to a conventional condenser. The impact of the choice of condenser on the price of power is calculated. Figures 1 and 2 show the coolant loops associated with the shell-and-tube and direct-contact condensers. In the shell-and-tube condenser, pentane condenses on the outside of tubes through which cool water is flowing. The cooling water absorbs heat and rejects it in the evaporative cooling tower. Noncondensable gases are continuously removed from the condenser. Before being vented to the atmosphere, they pass through the vent condenser where some of the pentane carried with them is condensed.

The direct-contact condenser subsystem is more complicated because the pentane and brine can contaminate each other. This subsystem includes a condenser and a vent condenser, as well as a deaerator and a degasser. The coolant is brine from the most concentrated of the evaporating ponds. Heat rejected into the evaporating pond speeds up the brine concentration process.

Brine is pumped from the evaporating pond through a deaerator. The deaerator is necessary in the direct-contact system to make the brine less corrosive, reduce the amount of air that will come out of solution and degrade condenser performance, and lessen the possibility of producing an explosive mixture of oxygen and pentane vapor in the condenser or degasser.

It is conservative to assume that the brine will

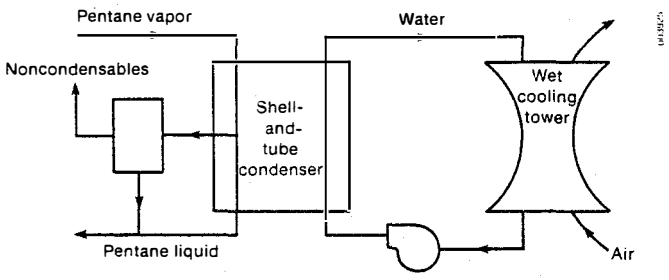

FIG. 1 SHELL-AND-TUBE CONDENSER SUBSYSTEM

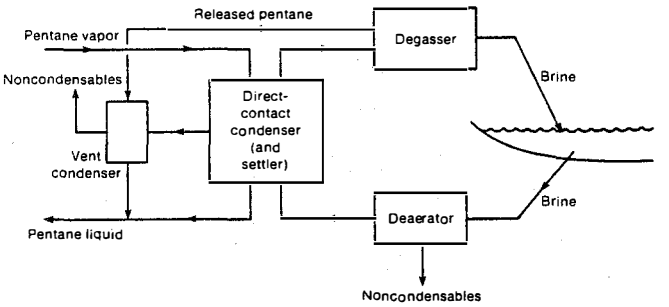

FIG. 2 DIRECT-CONTACT CONDENSER SUBSYSTEM

become saturated with pentane in the condenser and that any pentane entering the evaporating pond will be lost into the atmosphere. Although pentane is much less soluble in concentrated brine than in fresh water, it is not economically feasible to lose as much pentane as can be dissolved in brine at the condenser pressure. Therefore, a degasser must be inserted between the condenser and the evaporating pond to retrieve some of the dissolved pentane.

If the air above the surface of the evaporating pond is stagnant, the partial pressure of pentane, and thus the concentration of pentane in the layer of air nearest the surface, is related to the concentration of pentane in the brine by Henry's law. The degasser duty was determined by requiring that the pentane concentration in the air above the evaporating pond be below the lower explosive limit. This requirement is much stricter than necessary, since air motion over the cooling pond will quickly disperse the pentane vapor. The safety requirement reduces the cost of pentane lost to a small percentage of the plant's operating expenses.

METHOD OF COMPARISON

We first sized the four condenser subsystems so that each plant produces the same gross amount of electricity where pentane mass flow rate (115 kg/s) and turbine exit pressure (73.8 kPa) are held constant. The constraint on turbine exit pressure implies that the condensers have the same pressure at the pentane inlet. However, the pressure at which condensation occurs (taken as the average inside the condenser) is different for the different designs. There is a penalty for condensers that have large pressure drops: lowering the condenser pressure lowers the saturation temperature of the pentane and decreases the driving force for condensation. This decrease in driving force must be counterbalanced by an increase in area of contact or residence time, and thus by an increase in condenser size and cost.

We assumed the coolant is available at 20°C and chose coolant flow rates to give a reasonable pinch-point temperature difference in the condenser. The saturation temperature corresponding to the turbine exit pressure specified is 300 K (26.85°C), but the temperature at which condensation actually occurs may be up to 1°C lower due to pressure losses. To provide a minimum temperature difference of about 1°C, we selected 25°C as the coolant condenser exit temperature.

Because the effects of noncondensables on condenser performance are known for only some of the condenser options, we designed the condensers assuming that there were no noncondensables. Finally, we assumed that desuperheating takes place at the same rate as condensation.

SCALE-UP AND COSTING PROCEDURE

After sizing all four plants for 5-MW_e gross output, we compensated for the different parasitic losses, rescaled each plant to produce 5 MW_e net, and calculated the new capital and operating costs. When the entire plant is enlarged, the efficiency remains nearly constant because both the heat absorbed and the parasitic losses are directly proportional to the working fluid, hot brine, and coolant mass flow rates. Thus, efficiency is independent of size.

For a fair cost comparison, it is necessary to include the cost of the rest of the plant and of the solar pond scaled for the new flow rate. Instead of a detailed resizing of the entire plant, we applied the empirical "six-tenths rule" to the cost estimates provided by Wright (1,3) for the components of the plant other than the condenser subsystem. This empirical rule states that the ratio of the costs of two similar pieces of equipment is roughly equal to the ratio of their capacities raised to the six-tenths power. For the solar pond itself, we assumed that the cost is linearly dependent on the amount of heat removed. The cost of the evaporating pond associated with any of the direct-contact condensers will be less than that associated with a power plant that rejects heat into a cooling tower. However, the cost of the entire evaporating pond is a fairly small part of the cost of the entire system.

The final comparison is based on the cost of these scaled-up plants. If there is a substantial cost difference between one of the direct-contact subsystems and the shell-and-tube subsystem, this procedure should be sufficient to detect it. If the difference is not large, then this technique and optimization may give conflicting results. However, because of the many uncertainties associated with direct-contact design, the direct-contact subsystem will be competitive only if it is much less expensive than the conventional shell-and-tube subsystem.

RELATIONSHIPS USED IN SIZING CONDENSER SUBSYSTEMS

In this section, we present the methods used to size the components of the direct-contact and shell-and-tube condenser subsystems. The three direct-contact condensers under consideration are the drop-type, the bubble-type, and the packed-bed, shown in Figures 3, 4, and 5. In the bubble-type condenser, bubbles of pentane vapor condense into drops of pentane liquid as they rise through a continuous phase of brine. In the drop-type condenser, the pentane condenses in a thin film on falling droplets of brine. In the packed-bed condenser, it condenses in a thin film on a layer of brine that flows over packing.

Drop-Type Condenser

The brine stream passes through nozzles and enters

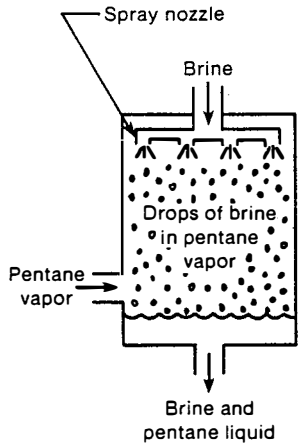

FIG. 3 ILLUSTRATION OF A DROP-TYPE CONDENSER

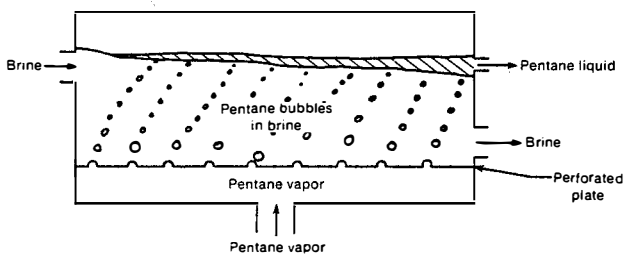

FIG. 4 ILLUSTRATION OF A BUBBLE-TYPE CONDENSER

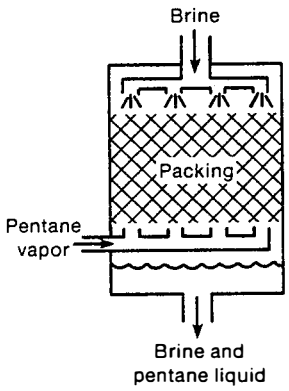

FIG. 5 ILLUSTRATION OF A PACKED-BED CONDENSER

the condenser as a spray of droplets. Pentane vapor from the turbine enters the condenser from the side and forms the continuous phase. Pentane vapor condenses on the drops, and the coolant and condensate collect at the bottom of the condenser. Then they travel to a settling tank where they are separated.

The size of the condenser is determined as follows. Heat transfer relationships specify the residence time required of the brine as a function of droplet radius and other condenser conditions. The residence time requirement can be converted to a height requirement using nozzle exit velocities and terminal velocity correlations. The cross-sectional area of the condenser is chosen on the basis of nozzle spacing. An average drop size can be predicted for given nozzles and pressure drops using information supplied by the spray nozzle manufacturer.

This condenser has the advantage of a low vapor-side pressure drop. Condensation is assumed to occur at the turbine exit pressure. Its disadvantage lies in the high parasitic losses. The brine has a large, non-recoverable head loss as it passes through the nozzles and as it falls through the pentane vapor. Another problem is that the brine and pentane must be separated after they leave the condenser.

The heat transfer relationships selected for this analysis were developed by Jacobs and Cook (4), using a theoretical model of a single, noncirculating drop that takes into account the resistance to heat transfer of the film of condensate. The model assumes that the condensation rate is controlled by conduction to the surface of the drop from within, the thermal capacitance of the condensate is negligible, and the condensate film has a linear temperature profile. A simplified energy balance and the conduction equation for the coolant drop are solved numerically.

The model treats drops as rigid, noncirculating spheres, an approximation that is accurate only for very small drops. Larger drops are likely to have internal circulation and a nonspherical shape that has larger surface area. Since both of these phenomena enhance heat transfer, the rigid, noncirculating sphere assumption is a conservative one. The model also neglects drop interactions and collisions. Collisions enhance heat transfer because they promote circulation within drops and because they sometimes result in an increase in surface area. However, some collisions end in the coalescence of the drops, decreasing the surface area. In addition, drops affect each other's velocity even when they do not collide. An ensemble of drops falls at a "hindered velocity," slower than the terminal velocity of a single drop. This increases the time available for heat transfer in a given height, but it also implies that the vapor undergoes a measurable pressure drop. Finally, the presence of other drops may hinder heat transfer. As they fall, some drops will be partially shielded by others from pentane vapor. Thus, the heat transfer process may be controlled by the availability of vapor rather than by the conduction rate through the drop. Therefore, it is not clear whether the single drop assumption is conservative or optimistic.

The height of a drop-type condenser is determined using heat transfer relationships and knowledge of the drops' velocities. For terminal velocities of liquid drops falling in gases, Clift, Grace, and Weber (5) recommend the correlation of Garner and Lihou, based on experimental data on liquid drops in air. Drop interactions and wall effects are negligible in the experiments used for their correlation. We modified this correlation slightly to account for deceleration from nozzle exit to terminal velocity.

Bubble-Type Condenser

In the bubble-type condenser, brine enters on one side near the top and flows out the other side near the bottom. Pentane enters a chamber below the brine and then passes through the holes of a sieve tray, forming bubbles in the brine. The bubbles condense as they rise and become drops of pentane liquid, which collect in a layer on the top of the brine. This layer leaves the condenser through its own outlet and is pumped to boiler pressure.

The sizing procedure for the bubble-type condenser is similar to that for the drop-type condenser. Heat transfer and bubble velocity relationships determine the condenser height required for heat transfer. The cross-sectional area is chosen to prevent flooding. Bubble size and pressure drop during bubble formation are predicted using the empirical correlations of

Mersmann (6) and Smith and Van Winkle (7), respectively.

The bubble-type condenser has the lowest parasitic losses of the three designs. Because the brine is in the continuous phase, the gravitational potential energy that it loses in moving downward in the condenser is recovered in the form of increased pressure. Furthermore, the pentane separates from the brine in the condensation process, removing the need for a settling tank. The disadvantage of the bubble-type condenser is that it has a high vapor-side pressure drop. Pentane must overcome the pressure drop across the orifice plate and the hydrostatic pressure of the brine above. Since all three designs are compared on the basis of constant turbine exit pressure, the high pressure drop decreases the driving force for condensation and increases the height of the condenser. This increases the pressure drop, so the process of determining condenser height is iterative. As bubble size increases, so does the height of the column of brine required for condensation. For bubbles larger than a certain size, it is impossible to maintain the turbine exit pressure at the desired level and at the same time achieve complete condensation. For that reason the condenser must be designed with small bubbles.

The considerable literature on condensation of vapor bubbles is reviewed in a recent article on direct-contact condensation (8). More recent work on bubble collapse includes the derivation of an analytical expression for the single-bubble case (9) that considers the thermal resistance of the condensate inside the bubble. The multibubble models predict a slower collapse rate than the single-bubble models because other bubbles make the water warmer around a given bubble, reducing the driving force for condensation. We used the single-bubble model for ease of analysis but compensated for the effects of other bubbles by using the average brine temperature to compute the driving force.

The single-bubble models described in Refs. (9) and (10) predict extremely rapid bubble collapse for our conditions. These models have not been directly confirmed by experiments, since the effect of noncondensable gases is significant in all reported experiments. However, when the model in Ref. (9) is expanded to account for noncondensables [Ref. (11)], it agrees very well with experimental results.

Making a theoretical prediction of the rise velocity of a condensing bubble is difficult, since both the size and the density of the bubble are changing. Furthermore, the problem is coupled to the heat transfer problem. However, experiments indicate that bubble rise velocity is nearly constant for pentane bubbles with initial radii between 2 and 4 mm, rising in water [Ref. (11)]. It is reasonable to expect the presence of other bubbles to slow bubble rise rather than hasten it. In this analysis we assumed that a bubble rises constantly at the terminal velocity associated with its initial properties. Clift, Grace, and Weber (5) recommend a correlation from Grace, Wairegi, and Nguyen for systems that are not exceptionally pure.

The cross-sectional area of the condenser must be large enough to keep flooding from occurring. Flooding takes place in a two-phase device in one of two ways. If the discontinuous-phase (i.e., pentane) flow rate is high, then particles of the discontinuous phase may crowd together and become the continuous phase. If the continuous-phase (i.e., brine) flow rate is high, it may entrain particles of the discontinuous phase.

To prevent the first form of flooding, it is necessary to establish the spacing of the bubbles when they are largest; i.e., as they leave the orifice plate. We required that the distance between holes in the orifice plate be at least twice the initial radius of a bubble. Because there is still some danger that consecutive bubbles from the same orifice may crowd together and combine, the cross-sectional area selected here should be regarded as a lower limit. It is important to avoid entrainment of pentane bubbles in the brine to minimize working fluid loss. If the pentane bubbles rise with a velocity V_T through a height Z, and the brine has a lateral velocity V_l at its exit, then any pentane bubbles formed within a radius of $(V_l Z)/V_T$ of the brine exit will be entrained. This means that the portion of the condenser within this radius cannot be used. For a given condenser cross-sectional area, the brine velocity can be reduced by increasing the height of the column of water or by providing more than one brine inlet and outlet orifice.

Packed-Bed Condenser

The third type of condenser consists of a column filled with packing. Brine enters the column from the top and forms a thin film on the packing. Pentane vapor enters from the bottom and condenses on the brine, and the brine and pentane liquid leave together from the bottom of the column. Heat transfer relationships are given in terms of a volumetric heat transfer coefficient, which determines the active volume of the condenser. The cross-sectional area is chosen to give a desired vapor-side pressure drop for the flow rates and type of packing under consideration. One advantage of this condenser design is that condensation occurs with the two fluids in counterflow. Another advantage is the low vapor-side pressure drop. The disadvantages are the necessity of separating the brine and pentane, and the fairly high parasitic losses. Parasitic losses occur because of the nonrecoverable head loss as the brine falls over the packing.

An experimental heat transfer correlation calculated by Jacobs, Thomas, and Boehm (12) is used in this analysis. They studied the condensation of R-113 on fresh water in a packed bed and compared their results to those of previous investigators' experiments on the condensation of steam on Aroclor and of methylene chloride on water. They correlated the data in terms of the following important dimensionless quantities: the Jakob number (the ratio of latent and sensible heat transfer), a modified Stanton number (relating heat transfer area and heat load), a dimensionless column height, and a ratio of the products of mass flow rates and specific heats for the vapor and coolant. Somewhat surprisingly, they found no dependence on the thermal conductivity of the condensate, although the experiments involved fluids with a large range of thermal conductivities.

To select the condenser cross-sectional area and calculate vapor-side pressure drop, we used plots provided by packing manufacturers that relate flow rates, areas, densities, viscosities, and pressure drops. For a given ratio of brine and pentane flow rates, pressure drop increases as area decreases. In general, larger packings give lower pressure drops for given flow rates and cross-sectional areas.

Deaerator and Degasser

The deaerator and the degasser have essentially the same design, since their function is the same: to remove a small quantity of dissolved material from the brine stream. The deaerator is a packed column maintained at low pressure. Brine enters the top of the deaerator and falls onto the packing, where it forms a thin film, facilitating gas desorption. The desorbed gas is vented to the atmosphere by compressors. The

degasser works exactly the same way; but the desorbed gas, mainly pentane, is returned to the condenser by compressors.

The desorption requirements are so stringent that the deaerator and degasser experience large parasitic losses, both from brine head loss and from the work of the compressors. The deaerator and degasser operate under the principle of Henry's law, which states that the equilibrium concentration of a sparsely soluble gas in a liquid is directly proportional to the partial pressure of the gas above the liquid. The constant of proportionality H for air in 25% salt water is approximately 4.18 ppm/atm.

The deaerator is maintained at a very low pressure P_{da} and the partial pressure of the air over the brine in the deaerator is $P_{da} - P_{brine}$, where P_{brine} is the saturation pressure of brine at that temperature. Thus, the equilibrium concentration of air in the brine in the deaerator is $X_{a_{eq}} = H (P_{da} - P_{brine})$ and can be reduced as much as desired by reducing the deaerator pressure. How close it comes to the equilibrium concentration depends on residence time, initial concentration, flow rate, and surface area exposed.

We used the correlation in Ref. (13) to predict the rate of approach to equilibrium. The correlation is based on experiments on the desorption of air from fresh water. It is expressed in terms of a height of transfer unit (HTU), related to the desorption rate as follows: the concentration X of a gas in the brine decays exponentially, approaching its equilibrium value. The desorption rate can be expressed by the equation

$$e^{-NTU} = \frac{X_{out} - X_{eq}}{X_{in} - X_{eq}} ,$$

where X_{in}, X_{out}, and X_{eq} are, respectively, the initial, final, and equilibrium concentrations of gas in the brine in the column. This equation serves as the definition of the number of transfer units (NTU). The HTU is the height of column required for one NTU. Figure 6 shows HTU versus cross-sectional area for the desorption of air and pentane from brine for the flow rate of interest.

Shell-and-Tube Condenser

The shell-and-tube condenser consists of a group of tubes inside a pressure vessel. The coolant (water) flows through the tubes, and the pentane vapor condenses on the shell side. We neglected any vapor-side pressure drop in the condenser under the assumption that it is very small in a well-designed condenser. The main source of parasitic losses for this type of condenser is the brine head loss due to friction with the tube wall. The shell-and-tube condenser is sized on the basis of a rough design, taking into account only the diameter and total surface area of the tubes. The surface area required for heat transfer is calculated from the overall heat transfer coefficient (14).

The mechanical draft cooling tower is a direct-contact counter-flow heat exchanger, in which the cooling water transfers heat to the air by evaporation as well as forced convection. Since cost correlations are available for cooling towers as a function of flow rates and temperatures (14), it is not necessary to size the cooling tower in any detail.

SIZE AND COST OF CONDENSER SUBSYSTEMS

The main design variable for the drop-type condenser is the drop size, which determines residence time and terminal velocity. Drop size increases with nozzle size for a given pressure drop, and decreases with pressure drop for a given nozzle. We considered only nozzles operating at the lowest pressure drop for which the manufacturer provided data (68.95 kPa or 10 psi) and had to choose among nozzles of different capacities. This choice involved a rough trade-off between condenser height (and thus gravitational parasitic losses) and condenser area (which depends on the number of nozzles). We selected a nozzle with a capacity of approximately 0.89 kg/s. The median drop diameter is 650 μm.

Heat transfer relationships gave a residence time requirement of 0.43 s for a 1.3-mm-diameter drop under the operating conditions of the condenser. This corresponds to an active height of 1.98 m. The condenser itself must be somewhat taller than this (3.0 m) to allow space for the spray nozzles and brine distribution system, but only the active height contributes to parasitic losses.

The cross-sectional area of the condenser is chosen on the basis of nozzle spacing. We arbitrarily chose to place the nozzles 25 cm apart, in an equilateral triangle. Since approximately 3000 spray nozzles are required, the condenser must have a cross-sectional area of 163 m^2. Since cost information is not readily available for pressure vessels of this size, and because such vessels would require expensive field fabrication, we chose to design this condenser (and other large system components) as a group of smaller units in parallel. Each unit has a diameter of 3.65 m (12 ft) or less, so that it can be transported by truck from the manufacturer to the plant site. The drop-type condenser will consist of 16 of these units.

The bubble-type condenser was designed for 6-mm bubbles, which require a cross-sectional area of 245 m^2. Like the drop-type condenser, this condenser will be built of smaller modules in parallel. Twenty-four modules are needed.

The height required for heat transfer for bubbles of this size is very small, but the condenser must be designed with a much taller column of brine to avoid substantial entrainment of pentane. We designed the condenser so that the lateral velocity of the brine at its outlets would be roughly the same as the rise velocity of the pentane bubbles. For a volumetric flow rate of 0.078 m^3/s per module, this leads to the requirement that the pentane exit pipe be at least 70 cm in diameter. To reduce the size of the pipe, we chose to have two brine outlets and two inlets, each with a diameter of 50 cm. The actual height of each module will be 1 m, with a generous allowance for the height of the vapor chamber and the layer of pentane liquid above the brine. Since this is fairly short, several modules can be stacked to form larger pressure vessels.

The correlation in Ref. (12) expresses heat transfer in terms of a volumetric heat transfer coefficient, but the correlation determines the height, not the volume, of the packed-bed condenser when it is put in dimensional form. Our design uses 3.81-cm (1.5-in.) Berl saddles. The column is designed for a pressure drop of 1.2 kPa/m of height (1-1/2 in. of water per foot of height) with a 10% safety factor in area. According to the heat transfer correlation, the condenser must have an active height of 2.95 m. According to flow-rate/pressure correlations, the condenser must have an area of 91 m^2. This corresponds to 9 modules.

In order to use the heat transfer correlations for shell-and-tube heat exchangers, we selected 2.0 cm as the tubes' external diameter, and 1.9 cm as the internal diameter (15). The tubes are made of carbon steel. The overall heat transfer coefficient calculated for these tubes is 1090 $W/m^2\ ^oC$, which is within the range given by Perry and Chilton (14) for organic vapors condensing on tubes containing water. The required surface area is 11,000 m^2.

Deaerator and Degasser

For a given deaeration load the active height and area of the deaerator are interrelated. The duty of the deaerator can be described as a number of transfer units (5.7 in this case) required to reduce noncondensables in the condenser to 1% by volume. The active height of the deaerator is the product of NTU and HTU. The sizing of the deaerator involves a trade-off between the cost of increasing area and the cost of the parasitics caused by a large active height. A rough calculation indicated that the least expensive design was the one with the smallest deaerator or degasser cross-sectional area permitted by flooding considerations.

Both the degasser and the deaerator use 2.54-cm (1-in.) plastic Pall rings as packing. According to the flooding calculations in Ref. (13), the maximum flow rate per unit area is 47.5 kg/s m^2, which corresponds to a cross-sectional area of 56.3 m^2. We applied a safety factor of 10% and arrived at a cross-sectional area of 62 m^2.

Because the deaerator and degasser operate at lower pressures than the following points in the brine loop, brine must be pumped out of them. To reduce pumping required, the brine enters the degasser and deaerator by barometric lift.

For the design conditions Figure 6 shows that the HTUs for air and pentane desorption are 1.14 m and 1.90 m, respectively. The NTUs set by the desorption requirements are 5.7 for air and 4.4 for pentane. This leads to a deaerator with an active height of 6.5 m, and a degasser with an active height of 8.4 m. These heights correspond to parasitic losses of 170.6 kW and 219.7 kW, respectively. The other source of parasitic loss is the work of the compressors that remove the desorbed gases and whatever water vapor is released.

PLANT EFFICIENCY

The parasitic losses of the four condenser subsystems and of the rest of the power plant are summarized in Table 1. Parasitic losses due to pipe friction are neglected since they should be the same for all the plant designs. The efficiency of each plant is listed in Table 2.

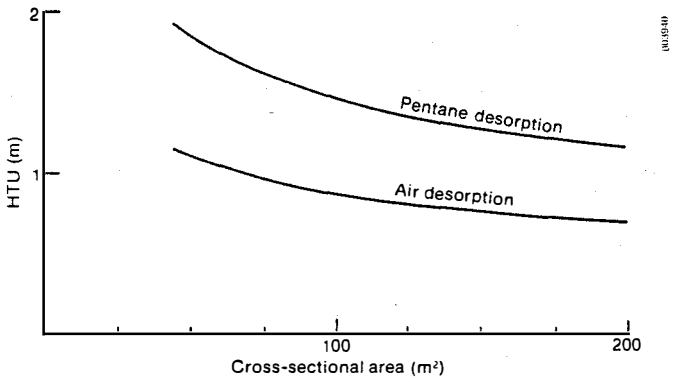

FIG. 6 HTU OF DEAERATOR AND DEGASSER

SCALE-UP: SIZING AND COSTING

The designs of condenser subsystem components are based on the same brine and pentane flow rates (2675.6 kg/s and 115 kg/s, respectively). For a fair evaluation of the condenser subsystem choices, each plant must be enlarged to produce the same net amount of electricity (5 MW_e). The scale-up procedure is used on the assumption that cycle efficiency is unchanged by a small change in the size of the plant.

Table 1. Parasitic Losses

Direct-contact condenser subsystems	
Deaerator	
Gravity head loss	213.2 kW
Compressor work	48.7 kW
Condensers	
Drop-type condenser	
Nozzle head loss	194.9 kW
Gravity head loss	65.0 kW
Bubble-type condenser	
Extra pumping for pentane liquid	1.3 kW
Packed-bed condenser	
Gravity head loss	96.8 kW
Degasser	
Gravity head loss	274.6 kW
Compressor work	13.1 kW
Shell-and-tube condenser subsystem	
Frictional head loss in shell-and-tube condenser	237.2
Gravity head loss in cooling tower	90.6
Work of fans in cooling tower	198.8
Total for drop-type condenser subsystem	809.5 kW
Total for bubble-type condenser subsystem	550.9 kW
Total for packed-bed condenser subsystem	646.4 kW
Total for shell-and-tube condenser subsystem	526.6 kW
Rest of the plant	
Work of pumping pentane from condenser to boiler	53.8 kW
Work of pumping brine from pond to boiler	256.4 kW
Total for the rest of the plant	310.2 kW

Table 2. Cycle Efficiency

Condenser	Useful Output (MW_e)	Net Efficiency (%)
Drop-type	4.293	8.43
Bubble-type	4.552	8.94
Packed-bed	4.456	8.75
Shell-and-tube	4.576	8.98

After scale-up, we used the costing method in Ref. (16) to estimate the cost of the direct-contact system components. The result of this costing procedure is an FOB cost (the total cost to be paid to the manufacturer before shipping) in 1980 dollars. These results are summarized in Table 3.

Cost for the scaled-up shell-and-tube subsystem are also given in Table 3. They were calculated assuming a cost of \$215/m^2 of tube area.

The cost of the shell-and-tube condenser subsystem could be reduced significantly if the cooling tower could be replaced by a cooling pond. This would reduce parasitics. The plant's efficiency would be 9.55%, which implies a condenser cost of \$2,430,000.

To calculate the scaled-up cost of the plant (excluding condenser subsystem) and pond, we applied the

Table 3. Cost of Subsystems (1980$)

	Number of Modules	Total Area (m^2)	Cost per Module ($)	Total Cost ($)
Drop-type				
Deaerator	7	72	100,700	705,100
Condenser	19	190	45,800	870,000
Settler	1		64,300	64,300
Degasser	7	72	118,300	828,100
Pumps	4		23,500	94,000
Compressors	2			65,000
Total				2,626,500
Bubble-type				
Deaerator	7	68	95,900	671,100
Condenser	7	270	72,600	508,400
Settler				
Degasser	7	68	112,600	787,900
Pumps	3		19,600	58,800
Compressors	2			65,000
Total				2,091,200
Packed-bed				
Deaerator	7	70	97,800	684,600
Condenser	10		59,500	595,100
Settler	1	102	64,300	64,300
Degasser	7	70	114,800	803,900
Pumps	4		18,300	73,100
Compressors	2			65,000
Total				2,286,000
Shell-and-tube				
Condenser	--	--	--	2,580,000
Pumps	--	--	--	28,800
Cooling tower	--	--	--	433,000
Total				3,041,800

six-tenths rule to a cost estimate of the power plant provided by Wright (1,3). Wright's estimate of the field cost ($4,364,000) is multiplied by a different scaling factor for each plant, and added to the cost of the condenser subsystem, as shown in Table 4. The field cost of the plant is converted to capital cost and added to the cost of the solar pond and the equivalent capital cost of pentane replacement.

If the year-round average incident solar radiation on the pond is 250 W/m^2, and 16% of this amount is stored in the pond, then energy can be extracted from the pond at a rate of 40 W/m^2. Cost estimates for solar ponds vary from $5/$m^2$ to $18/$m^2$, depending on whether a liner is used, how much construction work is required, and how large the pond is (17,18). We chose an intermediate value of $10/$m^2$.

CONCLUSIONS

Table 4 shows that the cost of the best direct-contact systems is 30% lower than that of the shell-and-tube system. However, the reduction in the cost of the entire power plant and pond is only 5%. In many cases the direct-contact power plant was more expensive because of its reduced efficiency. Because the uncertainty associated with the design is far less for shell-and-tube condensers than for direct-contact condensers, the shell-and-tube option would be preferable unless the direct-contact condenser subsystem were considerably less expensive. The direct-contact condenser subsystems, as designed, do not reduce the capital cost of the plant, pond, and pentane enough to justify the risks inherent in a relatively new technology.

It is important to note that the deaerator and degasser, not the condenser, account for the major part of the cost of the direct-contact condenser subsystem. The deaerator and degasser contribute between 63% and 75% to the cost of the condenser subsystem and are responsible for between 68% and 99% of the subsystem's parasitic losses. (The parasitic losses caused by pipe friction and the work of the compressors associated with the vent condenser are neglected.) Thus, the plant's efficiency would be increased significantly if

Table 4. Scaled-Up Costs of Power Plant and Solar Pond[a]

	Type of Condenser			
	Drop-Type	Bubble-Type	Packed-Bed	Shell-and-Tube
Scale-up factor for plant	1.096	1.058	1.071	1.055
Total field cost of plant excluding condenser subsystem	4,781	4,617	4,676	4,602
FOB cost of condenser subsystem	2,626	2,091	2,286	3,042
Total field cost of plant	7,408	6,708	6,962	7,644
Total capital cost of plant	12,898	11,669	12,121	13,309
Total capital cost of pond	14,833	13,982	14,290	13,916
Capitalized cost of pentane make-up	52	49	50	3
Total capital cost	27,783	25,700	26,461	27,228
Capital cost per kW_e	5.557	5.14	5.292	5.446
Plant efficiency (%)	8.43	8.94	8.75	8.98
Brine flow rate (kg/s)	3,116	2,939	3,002	2,300[b]
Pentane flow rate (kg/s)	134	126	129	126

[a]All costs are in 1980 K$.

[b]Fresh water.

the degasser and deaerator could be eliminated. Some types of deaerators and degassers may be less expensive and have smaller parasitic losses than the packed-bed design that we have considered here. A better design could possibly change the cost of direct-contact options and the conclusions of this report.

To understand the possible impact on plant cost of smaller deaerators and degassers, we estimated the cost of a plant with a bubble-type condenser and no deaerator or degasser. The cost of the condenser subsystem was reduced to approximately 20% of the cost of the shell-and-tube subsystem; the cost of the rest of the system was also reduced because of higher efficiency. The final cost was approximately 20% of the cost of the shell-and-tube heat exchange system.

Another major area of uncertainty lies in particle spacing and multiparticle effects in the bubble-type and drop-type condensers. The choice of bubble and spray-nozzle spacing was arbitrary. Table 3 shows the effect of changing this spacing. The cost of the condenser is roughly proportional to the cross-sectional area, and parasitic losses are independent of area. Thus, changing spacing will affect the cost of the condenser, but not of the other components, the pond, or the rest of the plant. Since the condenser cost is outweighed by the combined cost of deaerator and degasser, a moderate change in spacing is unlikely to change the conclusions of this paper.

REFERENCES

1. Wright, J. D., Sizing of Direct-Contact Preheater/Boilers for Solar Pond Power Plants, SERI/TR-252-1401, Golden, CO: Solar Energy Research Institute, May 1982.

2. Fisher, Elizabeth, and J. D. Wright, Direct-Contact Condensers for Solar Pond Power Production, SERI/TR-232-2164, Golden, CO: Solar Energy Research Institute, June 1984.

3. Wright, J. D., An Organic Rankine Cycle Coupled to a Solar Pond by Direct-Contact Heat Exchange--Selection of a Working Fluid, SERI/TR-631-1122R, Golden, CO: Solar Energy Research Institute; June 1981, revised June 1982.

4. Jacobs, Harold R., and Donald S. Cook, "Direct-Contact Condensation on a Noncirculating Drop," Proceedings of the 6th International Heat Transfer Conference, Toronto, Vol. 2, 1978, pp. 389-393.

5. Clift, R., J. R. Grace, and M. E. Weber, Bubbles, Drops, and Particles, New York, NY: Academic Press, 1978, 380 pp.

6. Mersmann, Alfons, "Design and Scale-up of Bubble and Spray Columns," Ger. Chem. Eng., Vol. 1, 1978, pp. 1-11.

7. Smith, P. L., and Matthew Van Winkle, "Discharge Coefficients through Perforated Plates at Reynolds Numbers of 400 to 3000," AIChE Journal, Vol. 4, No. 3, 1958, pp. 266-268.

8. Sideman, Samuel, and David Moalem-Maron, "Direct-Contact Condensation," Advances in Heat Transfer, Vol. 15, 1982, pp. 227-281.

9. Jacobs, H. R., Heimir Fannar, and George C. Beggs, "Collapse of a Bubble of Vapor in an Immiscible Liquid," Proceedings of the 6th International Heat Transfer Conference, Toronto, Vol. 2, 1978, pp. 383-387.

10. Isenberg, Jerrold, David Moalem, and Samuel Sideman, "Direct-Contact Heat Transfer with Change of Phase: Bubble Collapse with Translatory Motion in Single and Two Component Systems," Proceedings of the 4th International Heat Transfer Conference, Paris, Vol. 5, 1970, paper B2.5.

11. Jacobs, H. R., and B. H. Major, "The Effect of Noncondensible Gases on Bubble Condensation in an Immiscible Liquid," Transactions of the ASME, Vol. 194, 1982, pp. 487-492.

12. Jacobs, H. R., K. D. Thomas, and R. F. Boehm, "Direct-Contact Condensation of Immiscible Fluids in Packed Beds," Proceedings of the 18th Natinal Heat Transfer Conference, New York, NY: American Society of Mechanical Engineers, 1979, pp. 103-110.

13. Golshani, A., and F. C. Chen, Ocean Thermal Gas Desorption Studies, ORNL/TM-7438/V2, Oak Ridge, TN: Oak Ridge National Laboratory, Sept. 1981.

14. Perry, Robert H., and Cecil H. Chilton, Chemical Engineers Handbook, 5th edition, New York: McGraw-Hill, 1973.

15. Robertson, R. C., 1980 (Mar.), "Condensers," Sourcebook on the Production of Electricity from Geothermal Energy, edited by Joseph Kestin, DOE/RA/28320-2, Providence, RI: Brown University, Mar. 1980.

16. Pikulik, A., and H. Diaz, "Cost Estimating for Major Process Equipment," Chemical Engineering, 10 Oct. 1977, pp. 106-122.

17. Jet Propulsion Laboratory, Regional Applicability and Potential of Salt-Gradient Solar Ponds in the United States, DOE/JPL 1060-50, Vol. 2, JPL Publication 82-10, Vol. 2, Pasadena, CA: JPL, Mar. 1982.

18. May, E. Kenneth, Cécile M. Leboeuf, and David Waddington, Conceptual Design of the Truscott Brine Lake Solar Pond System, SERI/TR-253-1833, Golden, CO: Solar Energy Research Institute, Dec. 1982.